Collisional ^{3}He and ^{129}Xe Frequency Shifts in Rb–Noble-Gas Mixtures

Z. L. Ma, E. G. Sorte, and B. Saam

Phys. Rev. Lett. **106**, 193005 — Published 11 May 2011

DOI: 10.1103/PhysRevLett.106.193005

Collisional ^{3}He and ^{129}Xe frequency shifts in Rb–noble-gas mixtures

Z. L. Ma, E. G. Sorte, and B. Saam*
Department of Physics and Astronomy,
University of Utah, 115 South 1400 East,
Salt Lake City, Utah, 84112-0830, USA

Abstract

The Fermi-contact interaction that characterizes collisional spin exchange of a noble gas with an alkali-metal vapor also gives rise to NMR and EPR frequency shifts of the noble-gas nucleus and the alkali-metal atom, respectively. We have measured the enhancement factor κ_0 that characterizes these shifts for Rb-^{129}Xe to be 493±31, making use of the previously measured value of κ_0 for Rb-^{3}He. This result allows accurate ^{129}Xe polarimetry with no need to reference a thermal-equilibrium NMR signal.

The study of hyperpolarized noble gases generated by spin-exchange optical pumping (SEOP) [1] continues to be vital and integral to recent work in many other fields, including condensed matter physics [2], materials science [3], and medical imaging [4, 5]. A fundamental aspect of SEOP physics is the collisional Fermi-contact hyperfine interaction $\alpha\mathbf{K}\cdot\mathbf{S}$ between the noble-gas nuclear spin $\mathbf{K}$ and the alkali-metal electron spin $\mathbf{S}$, where α is the coupling strength. This interaction is not only responsible for spin-exchange hyperpolarization of noble gases, but it also gives rise to complementary shifts in both the NMR frequency of the noble gas and the EPR frequency of the alkali-metal vapor that are proportional to the electron and nuclear magnetizations, respectively [6, 7]. These shifts provide insight into the nature of the interatomic potentials that ultimately determine spin-exchange rates for a given alkali-metal–noble-gas pair. If properly calibrated, the EPR shift also offers a simple and robust means to do noble-gas polarimetry in a typical low-field (few gauss) SEOP apparatus. The enhancement factor κ_0 that characterizes the frequency-shift calibration has been successfully measured for Rb-^{3}He to about 2% [8, 9] but until now was known to only about 50% for Rb-^{129}Xe [6]. The Rb-^{129}Xe measurement presents several method-dependent challenges, among them the fact that, unlike helium, high densities of xenon are difficult to polarize by SEOP. Indeed, the current lean-xenon flow-through method for generating large quantities of highly polarized ^{129}Xe [10, 11] would benefit greatly from a more precise measurement of κ_0 for Rb-^{129}Xe. In this work, we make consecutive measurements of the NMR shifts of both ^{3}He and ^{129}Xe at 2 T in the same glass cell under steady-state SEOP conditions. In cells having relatively low Xe density ([Xe] $\lesssim$ 10 Torr at 20 °C) we use the ratio of these shifts to deduce a much more precise temperature-independent value,

$$(\kappa_0)_{\mathrm{RbXe}} = 493 \pm 31, \tag{1}$$

from the known value of $(\kappa_0)_{\mathrm{RbHe}}$. In cells having [Xe] approx. ten times greater we observed an anomalous depression ($\approx 20\%$) of the shift ratio at the highest temperatures.

Averaged over many collisions, the interatomic hyperfine coupling results in a NMR frequency shift [6],

$$\Delta\,|\nu_X| = -\frac{1}{h}\frac{|\mu_K|}{K}\frac{8\pi}{3}\mu_B g_S \kappa_{XA}[A]\langle S_z\rangle, \tag{2}$$

where X is the noble gas species, h is Planck's constant, μ_K is the nuclear magnetic moment, μ_B is the Bohr magneton, $g_S \approx 2$ is the Landé factor, $[A]$ is the alkali-metal number density, and $\langle S_z \rangle$ is the volume-averaged expectation value of the z-component of the alkali-metal electron spin (in units of $\hbar$). The dimensionless factor κ_{XA} accounts for the enhancement of $\Delta\nu_X$ over the value it would have if the electron-spin magnetization were distributed continuously across a spherical sample. An equation complementary to Eq. (2) yields the EPR shift $\Delta\nu_A$ of the alkali-metal electron in the presence of the nuclear magnetization (proportional to $[X]\langle K_z \rangle$) with enhancement factor κ_{AX}. In the limit of high gas densities [12] that holds for all of this work, i.e., the regime in which binary collisions and short-lived van der Waals molecules dominate, $\kappa_{XA} = \kappa_{AX} \equiv \kappa_0$ for both Rb-^{3}He and Rb-^{129}Xe [6]. Eq. (2) is valid in this regime because the Rb spin is only slightly reoriented in a single interaction. Moreover, an applied magnetic field several times the spin-orbit field further suppresses electron reorientation in *all* molecules.

A direct measurement of $(\kappa_0)_{\mathrm{RbXe}}$ using Eq. (2) requires a measurement of the Rb magnetization (proportional to $[\mathrm{Rb}]\langle S_z \rangle$). To avoid this and substantially simplify the experiment, we form the ratio

$$(\kappa_0)_{\mathrm{RbXe}} = (\kappa_0)_{\mathrm{RbHe}} \left(\frac{\gamma_{\mathrm{He}}}{\gamma_{\mathrm{Xe}}}\right) \left(\frac{2\Delta\nu_{\mathrm{Xe}}}{2\Delta\nu_{\mathrm{He}}}\right), \tag{3}$$

where γ_X are the noble-gas gyromagnetic ratios and $2\Delta\nu_{\mathrm{X}}$ are the shifts in the respective noble-gas NMR frequencies when the Rb vapor is exactly flipped from the low- to the high-energy Zeeman polarization state (LES and HES, respectively); $|[\mathrm{Rb}]\langle S_z \rangle|$ is presumed to remain constant under steady-state SEOP conditions. We note that "LES" and "HES" will be used strictly in reference to the Rb polarization state and never to that of the ^{3}He or ^{129}Xe. In this work, we measure directly the frequency-shift ratio in Eq. (3), averaging many measurements to reduce the statistical uncertainty. We then multiply by the previously measured $(\kappa_0)_{\mathrm{RbHe}} = 4.52 + 0.00934T$ [8] (presumed valid over our temperature range), where T is the temperature in °C, to deduce $(\kappa_0)_{\mathrm{RbXe}}$.

Measurements were made on six d=7 mm i.d. sealed uncoated Pyrex-glass spheres containing a few milligrams of naturally abundant Rb metal along with ^{3}He, Xe (enriched to 86% ^{129}Xe), and N_2 in the various ratios shown in Table I. The cells are broadly divided into two categories containing high (50-100 Torr) and low (5-10 Torr) partial pressures of Xe. Spheres were used because Eq. (3) is strictly valid only for the case of a uniform spherical distribution of Rb magnetization for which the net average through-space dipole field is everywhere zero; effects due to imperfect geometry will alter the ^{3}He shift only, because $(\kappa_0)_{\mathrm{RbHe}}$ is on the order of unity, whereas $(\kappa_0)_{\mathrm{RbXe}}$ is two orders of magnitude larger. The small "pull-off" volume that results from cell fabrication (1-3% of the total cell volume in our case) and an inhomogeneous laser intensity through the cell can both give rise to nonspherical Rb magnetization. We note that geometrical shifts due to the nuclear magnetizations are less significant: rapid diffusion (compared to spin exchange) more readily guarantees a near-spherical distribution. We have determined through a combination of numerical modeling and experimentation that geometrical shifts amounted to no more than a 1-2% effect in even the most extreme cases.

NMR free-induction decays (FIDs) were acquired at 67.6 MHz (^{3}He) and 24.5 MHz (^{129}Xe) in a horizontal-bore 2 T superconducting magnet (Oxford). The Apollo (Tecmag) console is equipped with room-temperature shims and a gradient-coil set for imaging. The probe is a 35 mm diam Helmholtz coil immersed, along with the cell, in a safflower-oil bath contained in an Al-block reservoir with a plate-glass window to admit laser light. The probe could be tuned *in situ* from one nucleus to the other by manually switching in/out additional capacitance without otherwise disturbing the apparatus. The Al block was heated with air that flows past an external filament heater. The IR-transparent oil bath reduced temperature inhomogeneity across the cell (observed with the laser on to be as large as 20 °C in a flowing-air oven) to < 1 °C. A 30 W diode-laser array model A317B (QPC Lasers), externally tuned to the 795 nm D_1 resonance and narrowed to ≈ 0.3 nm with a Littrow cavity [13], was mounted on an optical table with the optical axis aligned with the magnet bore (and the cell) for SEOP; the maximum narrowed output was ≈ 20 W. The quarter-wave plate in the optical train was mounted in such a way as to allow precise and reproducible manual rotation of 180° about the vertical axis through its optical post, in order to rapidly reverse the Rb magnetization—this is accomplished in a time on the order of the characteristic optical pumping rate (a few tens of microseconds) after the waveplate has been flipped around; in practice the reversal takes ≈ 0.5 s.

Prior to data acquisition, SEOP was performed on the cell for a time $\gtrsim 1$ h, sufficient to build up polarization in both nuclear species. An auto-shimming procedure was performed with the laser blocked using the ^{3}He frequency spectrum to narrow the resonance line to ≈ 5 Hz. After unblocking the laser and allowing a SEOP steady state to be established, two FIDs were acquired with an intervening Rb magnetization reversal. This basic procedure took < 1 s to perform, minimizing the effects of static-field drift; it was then repeated ≈ 15 times before switching to the other nucleus. Provided $|[\mathrm{Rb}]\,\langle S_z \rangle|$ remains constant

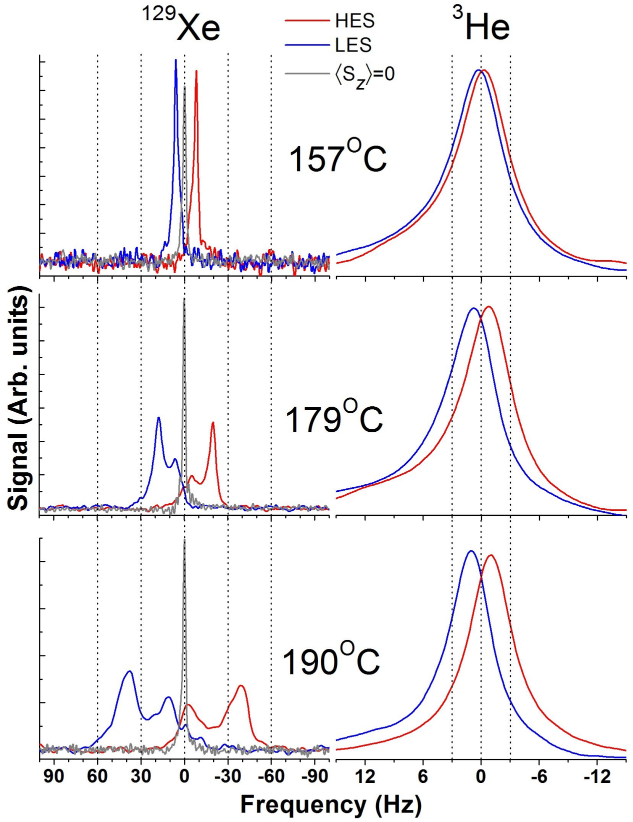

FIG. 1. (Color online) Typical ^{3}He and ^{129}Xe spectra (shown prior to apodization) from cell 155B acquired one-after-the-other under steady-state SEOP conditions. The narrow ^{129}Xe peak at 0 Hz was acquired with the laser blocked; it has been amplitude-normalized to appear on the same graph. The double peak in the ^{129}Xe spectra at all but the lowest temperatures represents regions of highly polarized and nearly unpolarized Rb vapor; the lines are broadened and begin to coalesce due to diffusion of ^{129}Xe between these two regions. For ^{3}He, the much smaller frequency-shift dispersion and more rapid diffusion yeilds a single narrow peak in all cases. The respective shifts in the spectral COM upon reversal of the Rb magnetization were used in Eq. (3) to extract $(\kappa_0)_{\mathrm{RbXe}}$.

throughout the measurement, the resulting frequency spectra yield ^{3}He and ^{129}Xe shifts suitable for use in Eq. (3), although the analysis has several subtleties.

The ^{129}Xe spectra in Fig. 1 have a characteristic two-peak structure for both the HES and LES compared to the narrow single peak acquired with the laser blocked (^{129}Xe still hyperpolarized but Rb unpolarized). In most cases, and particularly at higher temperatures, [Rb] $\langle S_z \rangle$ is inhomogeneous due to lensing and attenuation of the laser light as it propagates through the cell; the spectrum is essentially a one-dimensional projection of the NMR fre-

Cell	Xe:N_2:He (Torr)	$(\kappa_0)_{\mathrm{RbXe}}$
155A	5:160:2200	495±6
155B	10:250:2300	490±5
155C	10:168:2300	530±9
150A	50:175:1000	–
150B	110:350:2040	–
155D	50:172:1200	–

TABLE I. Summary of cell contents. All cells are sealed 7 mm i.d. uncoated Pyrex spheres. Quoted pressures are referenced to 20 °C and the Xe pressure is subject to $\approx 50\%$ uncertainty due to the filling procedure. $(\kappa_0)_{\mathrm{RbXe}}$ is computed for each of the low-[Xe] cells from the weighted average of that cell's data; we have excluded the high-[Xe] cells because of their anomalous behavior at high temperature.

quency shift due to this inhomogeneous distribution of [Rb] $\langle S_z \rangle$. However, the shape is also affected by diffusion. Diffusion of Xe is fast enough on the time scale of the FID that a given spin sees at least a partial average of frequency shifts. We hypothesize that the two-peak structure for ^{129}Xe emerges as [Rb] increases due to the abrupt transition in the cell between fully polarized and nearly unpolarized Rb [1]. We thus observed substantial fractions of the cell volume at the highest temperatures where the Rb polarization was quite low. The situation is not unlike chemical exchange (resonant nuclei sampling two chemically distinct sites during the FID), where the spectrum changes from two distinct peaks in the limit $\tau_s \Delta\omega \gg 1$ to a single motionally narrowed peak in the opposite limit. Here, τ_s is the sampling time between sites and is analogous to the diffusion time τ_d across the cell; $\Delta\omega$ is the difference in frequency for the two sites, analogous to the frequency difference between ^{129}Xe in contact with polarized and unpolarized Rb. In our ^{129}Xe data it is often the case that $\tau_d \Delta\omega \gtrsim 1$; for ^{3}He, with faster diffusion and a much smaller frequency-shift dispersion, we have $\tau_d \Delta\omega \ll 1$, corresponding to a single-peak spectrum (see Fig. 1).

The analysis of spectra like those in Fig. 1 rests on the condition that the noble-gas magnetizations are uniform across the cell at all times, i.e., that the diffusion time across the cell τ_d is much shorter than the spin-exchange time for each species, a condition always satisfied for ^{3}He. For ^{129}Xe we measured the diffusion coefficient using a standard pulsedgradient technique [14] to be $D_{\mathrm{Xe}} = 0.53 \pm 0.05$ cm^2/s in cell 150A at 170 °C. We thus have $\tau_d \approx d^2/6D_{\mathrm{Xe}} \approx 150$ ms. The measured value of the spin-exchange time for ^{129}Xe was at least 1-2 s in all cases and much longer at lower temperatures. We acquired ^{129}Xe magnetic resonance images of cell 150A at 170 °C that further verified the homogeneity of the nuclear magnetization, assuring that all Rb spins in the cell are weighted equally in the NMR spectrum. The shift in the spectral "center of mass" (COM) that occurs when the Rb magnetization is flipped thus corresponds to the volume-averaged frequency shift. The ^{129}Xe FIDs are multiplied by an apodizing exponential with a characteristic decay time about four times smaller than that of the FID. The subsequent fast Fourier transform produces a single broad symmetric spectral line that peaks at the spectral COM, the value of which is unchanged by the apodization procedure. As the raw ^{3}He spectra already consist of a single symmetric peak, they need no further analysis prior to measuring the shift. Thus, the shifts $\Delta\nu_{\mathrm{He}}$ and $\Delta\nu_{\mathrm{Xe}}$ are determined by comparing the respective HES and LES spectra and measuring the shift in a single peak.

Regarding this analysis we note the following: 1) The volume-averaged frequency shift is independent of sampling-time regime $\tau_s\Delta\omega$. 2) Our laser spectrum was narrow enough (≈ 140 GHz) that the optical pumping was affected by the ≈ 75 GHz Zeeman shift of the D_1 resonance in a 2 T field for $\sigma+$ compared to $\sigma-$ light. To correct for this effect we either made a small wavelength adjustment after flipping the quarterwave plate or broadened the laser to $\approx$950 GHz. The symmetry of the HES and LES spectra was used as an indicator that the adjustment had been made properly. 3) Rapid spin exchange attenuates/inverts the ^{129}Xe magnetization upon Rb-magnetization reversal; we verified that this has no effect on the spectral COM.

The calculated values of $(\kappa_0)_{\mathrm{RbXe}}$ are plotted vs. temperature T for the three low-[Xe] cells in Fig. 2a and for the three high-[Xe] cells in Fig. 2b. The error bars shown reflect only the statistical uncertainty in the measured frequency-shift ratio and do not include the uncertainty in $(\kappa_0)_{\mathrm{RbHe}}$; they are dominated by the large relative uncertainty in the small ^{3}He frequency shifts. The low-[Xe] cells (both individually and collectively) show no significant temperature dependence between 140-220 °C; the weighted average of all of these points yields an uncertainty of $< 1\%$. If we take the same weighted average on a cell-by-cell basis, there is a larger spread (see Table I), suggesting some unknown systematic errors at the few-percent level: these could include, for example, small cell-dependent geometrical effects.

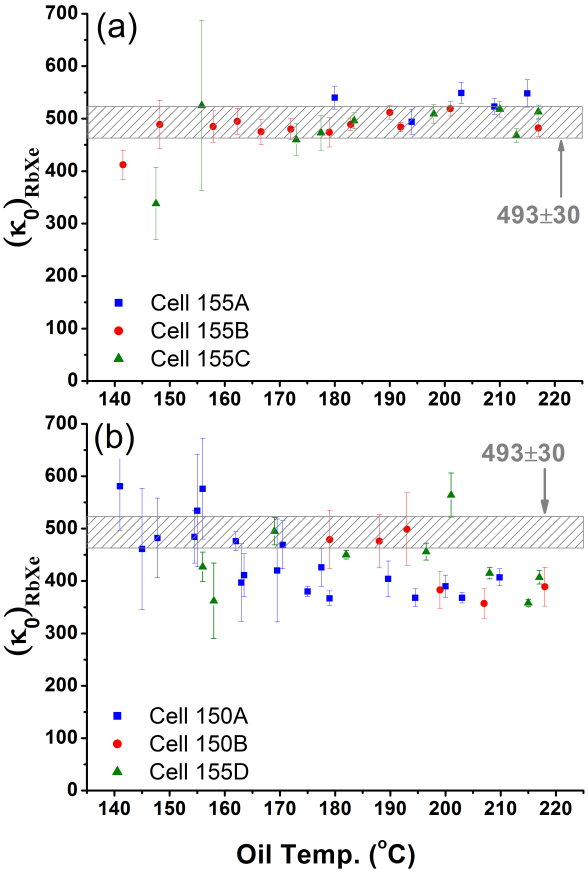

FIG. 2. Enhancement factor $(\kappa_0)_{\mathrm{RbXe}}$ plotted vs. temperature for (a) three low-[Xe] cells and (b) three high-[Xe] cells. The weighted average of all the low-[Xe] data points in (a) is 493, with the estimated uncertainty shown by the hatched region. We take these temperature-independent data to represent the best estimate of $(\kappa_0)_{\mathrm{RbXe}}$. The identical hatched region is shown in (b) for comparison: the high-[Xe] data are consistent with the low-[Xe] data up to about 175 °C; the $\approx 20\%$ drop-off at the highest temperatures is not understood.

In some cases, residual asymmetries are apparent in the HES and LES ^{129}Xe spectra with respect to the unpolarized-Rb peak (Fig. 1). These may be due to imperfections or drifts in laser tuning or power and may introduce some additional error at the $\approx 1\%$ level, although we found the two spectral COMs to be equidistant from the unpolarized-Rb peak in all cases. We accordingly increased the uncertainty in the shift ratio, which is represented by the hatched range in Fig. 2a. Finally, we add the 1.8% uncertainty in the value of $(\kappa_0)_{\mathrm{RbHe}}$ [8] in quadrature to this range to arrive at our final result in Eq. (1).

Below $T \approx 175$ °C, the data for the high-[Xe] cells are generally consistent with the hatched range (reproduced in Fig. 2b for comparison) that characterizes the low-[Xe] data. However, at the highest temperatures the measured shift ratio drops by about 20%. These ten or so data points out of 60 acquired for all 6 cells are at the extremes of high temperature, high [Rb], and rapid Rb spin destruction (due to higher [Xe]); yet we are unable to connect these physical conditions in a plausible way to the observed systematic depression of the shift ratio. We considered whether fast Rb-^{129}Xe spin exchange might lead to a violation of our fundamental assumption of uniform nuclear magnetization, but this would *increase* the shift ratio by preferentially weighting the regions of higher Rb magnetization in the ^{129}Xe spectrum. We also tested for extreme geometrical effects by remeasuring the shift ratio for both high- and low-[Xe] cells at a given temperature after significantly decreasing the laser power. The ^{129}Xe spectrum changed dramatically under these conditions, but the shift ratio was unchanged within error. We note that this test also served as a check on the robustness of the COM data-analysis method. The anomalous high-[Xe] high-temperature data points were excluded from the analysis because they are neither consistent from cell to cell nor consistent with a plausible theoretical temperature dependence.

We take the global average of the low-[Xe] data, 493±31, as our best estimate of $(\kappa_0)_{\mathrm{RbXe}}$. By comparison, Schaefer *et al.* [6] calculated $(\kappa_0)_{\mathrm{RbXe}} = 726$ and measured $(\kappa_0)_{\mathrm{RbXe}} = 644$ by mapping the ^{129}Xe NMR spectrum with the Rb EPR shift at low field. The uncertainty was reported in both the calculated and measured values as 30-40%. However, they were able to measure the ratio $\frac{(\kappa_0)_{\mathrm{RbXe}}}{(\kappa_0)_{\mathrm{RbKr}}} = 2.38 \pm 0.13$ at 90°C much more precisely and, to the extent that $(\kappa_0)_{\mathrm{RbKr}}$ is independent of temperature, we obtain $(\kappa_0)_{\mathrm{RbKr}} = 207 \pm 17$. Indeed, the theory that Schaefer *et al.* [6] present favors a zero to weakly positive temperature dependence for both $(\kappa_0)_{\mathrm{RbXe}}$and $(\kappa_0)_{\mathrm{RbKr}}$.

The authors are grateful to T. G. Walker and G. Laicher for helpful discussions. This work was supported by the National Science Foundation (PHY-0855482).

---

[*] saam@physics.utah.edu

[1] T. G. Walker and W. Happer, Rev. Mod. Phys. **69**, 629 (1997).

[2] S. W. Morgan, B. V. Fine, and B. Saam, Phys. Rev. Lett. **101**, 067601 (2008).

[3] L. Q. Wang, D. Wang, J. Liu, G. J. Exarhos, S. Pawsey, and I. Moudrakovski, J. Phys. Chem. C **113**, 6577 (2009).

[4] D. A. Yablonskiy, A. L. Sukstanskii, J. C. Woods, D. S. Gierada, J. D. Quirk, J. C. Hogg, J. D. Cooper, and M. S. Conradi, J. Appl. Phys. **107**, 1258 (2009).

[5] B. Driehuys, H. E. Möller, Z. I. Cleveland, J. Pollaro, and L. W. Hedlund, Radiology **252**, 386 (2009).

[6] S. R. Schaefer, G. D. Cates, T.-R. Chien, D. Gonatas, W. Happer, and T. G. Walker, Phys. Rev. A **39**, 5613 (1989).

[7] S. Appelt, A. B.-A. Baranga, C. J. Erickson, M. V. Romalis, A. R. Young, and W. Happer, Phys. Rev. A **58**, 1412 (1998).

[8] M. V. Romalis and G. D. Cates, Phys. Rev. A **58**, 3004 (1998).

[9] A. S. Barton, N. R. Newbury, G. D. Cates, B. Driehuys, H. Middleton, and B. Saam, Phys. Rev. A **49**, 2766 (1994).

[10] I. C. Ruset, S. Ketel, and F. W. Hersman, Phys. Rev. Lett. **96**, 053002 (2006).

[11] B. Driehuys, G. D. Cates, E. Miron, K. Sauer, D. K. Walter, and W. Happer, Appl. Phys. Lett. **69**, 1668 (1996).

[12] X. Zeng, Z. Wu, T. Call, E. Miron, D. Schreiber, and W. Happer, Phys. Rev. A **31**, 260 (1985).

[13] B. Chann, I. Nelson, and T. G. Walker, Opt. Lett. **25**, 1352 (2000).

[14] E. O. Stejskal and J. E. Tanner, J. Chem. Phys. **42**, 288 (1964).